Orbital: The Electronic Journal of Chemistry
journal homepage: www.orbital.ufms.br
e-ISSN 1984-6428

| Vol 12 | | No. 3 | | July-September 2020 |

FULL PAPER

DFT-QTAIM Study of Gold Nanoparticles and Cyclic Peptide as Effective Drug Nanocarriers

Bahareh Khoshbayan[a], Ali Morsali[a,b*], Safar Ali Beyramabadi[a,b], and Mohammad Reza Bozorgmehr[a,b]

[a]Department of Chemistry, Mashhad Branch, Islamic Azad University, Mashhad, Iran
[b]Research Center for Animal Development Applied Biology, Mashhad Branch, Islamic Azad University, Mashhad 917568, Iran

Article history: Received: 30 June 2020; revised: 24 July 2020; accepted: 01 august 2020. Available online: 30 September 2020. DOI: http://dx.doi.org/10.17807/orbital.v12i3.1519

Abstract:

In this study, cyclic peptide (CP) with cyclooctaglycine model and gold nanoparticles (AuNP) with Au6 cluster model were used to examin the function of penicillamine (PCA) drug on ten different configurations of cyclic peptide-gold nanoparticles (CPAuNP). Binding energies, quantum molecular descriptors such as electrophilicity power (ω), global hardness (η), and solubility energies were studied in aqueous solution and gas phase at the M06-2X density functional level. The binding energy analysis was performed on (CPAuNP/PCA1-10) structures to determine the most stable structure. The obtained values for solvation energies indicate that CPAuNPs can have an effective performance when used along with PCA drug, which is a major factor in drug delivery. The quantum molecular descriptors reveal that the reactivity of cyclic peptide (CP) and PCA drug increases in (CPAuNP/PCA1-10) structures. AIM calculations for all structures show that intermolecular hydrogen bonding and Au-L (L = H, O, S, C, N) interactions play an important role for this drug delivery system. When the PCA drug is parallel to the CPAuNP carrier, interacting simultaneously with CP and AuNP, the structure is more stable than the structures in which the drug has interactions only with the CP or AuNP.

Keywords: AIM analysis; density functional theory; penicillamine; quantum molecular descriptors

1. Introduction

The use of nanoparticles in drug delivery targeting is associated with a number of advantages including reducing the side effects of medications caused by targeted drug transfer, and also preventing their distribution to other healthy organs of the body [1, 2]. From among nanoparticles, the therapeutic application of gold nanoparticles has received considerable attention from researchers and authorities alike, mainly due to their unique optical, physical, and quantum characteristics, their high chemical stability, their easy synthesis, and their high viability properties [3-6]. Because gold nanoparticles enjoy high binding capability with many proteins and drugs actively targeting cancer cells, they are commonly employed in chemotherapy [7, 8].

In recent years, gold nanoparticles along with cyclic peptides (CPAuNPs) have been implemented as drug carriers in anticancer drugs [9]. Recently, cyclic peptides have been used as drug transporters for therapeutic purposes. Compared to their linear counterparts, these structures enjoy the ability to pass through the cell membrane more easily [10, 11].

Currently, cyclic peptides are believed to have potential applications in biology and chemistry, effectively implemented in a wide variety of fields including molecular transport systems, antibacterial agents [16,17], electronics, and the like. In addition to the laboratory methods, the quantum mechanical approach can be employed in the investigation of drug carrier systems [22-30].

*Corresponding author. E-mail: almorsali@yahoo.com

In the present study, the density functional theory (DFT) has been implemented to examine the potential positive effect of gold nanoparticles-cyclic peptides (CPAuNPs) used along with the penicillamine anticancer drug (PCA), which is commonly used for the treatment of the genetic disorder associated with copper metabolism (Wilson's Disease), and also as an anticancer agent in the treatment of cancer [31-33].

2. Results and Discussion

In this work, a number of important values such as binding energies, solvation energies, quantum molecular descriptors and charge density properties were used to examine the different types of interactions. In the present study, gold nanoparticles (Au_6 model) and cyclic peptide (cyclooctaglycine model) were used along with a penicillamine drug (PCA) containing SH, OH, CO and NH_2 groups to investigate the interaction of gold nanoparticles-cyclic peptide with penicillamine drug from ten different directions in aqueous solution phase. The Optimized Structures (PCA), (AuNP), (CP) and (CPAuNP/PCA1-10) at the M06-2X/6-31G(d,p) level are shown in Figs. 1-3. The following equation was used to determine the Binding energies (ΔE) of the different structures:

$$\Delta E = E_{CPAuNP/PCA1-10} - (E_{CP} + E_{AuNP} + E_{PCA}) \quad (1)$$

Table 1. Binding (ΔE) and solvation energies (ΔE_{solv}) for all structures (kJ mol^{-1})

Species	ΔE_{gas}	ΔE_{H2O}	ΔE_{solv}
PCA	-	-	-31.35
CP	-	-	-92.23
AuNP	-	-	-24.43
CP/PCA	-167.29	-140.19	-96.47
AuNP/PCA	-70.08	-61.46	-47.15
CPAuNP/PCA1	-260.01	-271.66	-159.65
CPAuNP/PCA2	-218.98	-230.60	-159.62
CPAuNP/PCA3	-284.17	-247.59	-111.42
CPAuNP/PCA4	-297.05	-266.71	-117.66
CPAuNP/ PCA5	-272.95	-239.63	-114.68
CPAuNP/ PCA6	-216.61	-223.91	-155.30
CPAuNP/ PCA7	-237.08	-241.96	-152.88
CPAuNP/ PCA8	-232.44	-205.59	-121.14
CPAuNP/ PCA9	-253.53	-253.50	-147.97
CPAuNP/PCA10	-200.37	-197.14	-144.77

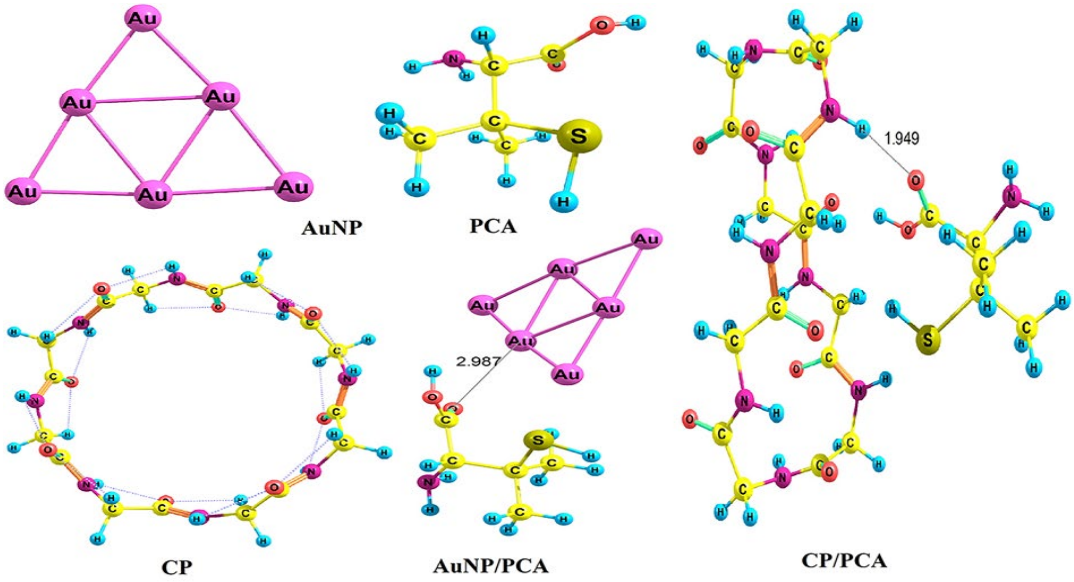

Figure 1. Optimized structures of AuNP, PCA, CP, CP/PCA and AuNP/PCA in aqueous solution at M062X/6-31G**.

Table 1 summarizes the binding energies in the gas phase and the aqueous solution at M06-2X level. The most stable structure in the solution phase is CPAuNP/PCA1, which has a more negative binding energy in this phase than the gas phase. CPAuNP/PCA2, CPAuNP/PCA6 and CPAuNP/PCA7 behave similarly to CPAuNP/PCA1, but on average the structures in the gas phase (-247.3 kJ mol^{-1}) are slightly more stable than those in the solution phase (-237.8 kJ

mol^{-1}) due to the competition of solvent molecules with the drug to bind to the carrier. As mentioned recently, in the aqueous solution, CPAuNP/PCA1 is the most stable configuration, with penicillamine drug being parallel to CPAuNP, and the C=O functional group of CPAuNP interacting with the OH functional group of the PCA drug through the hydrogen bond.

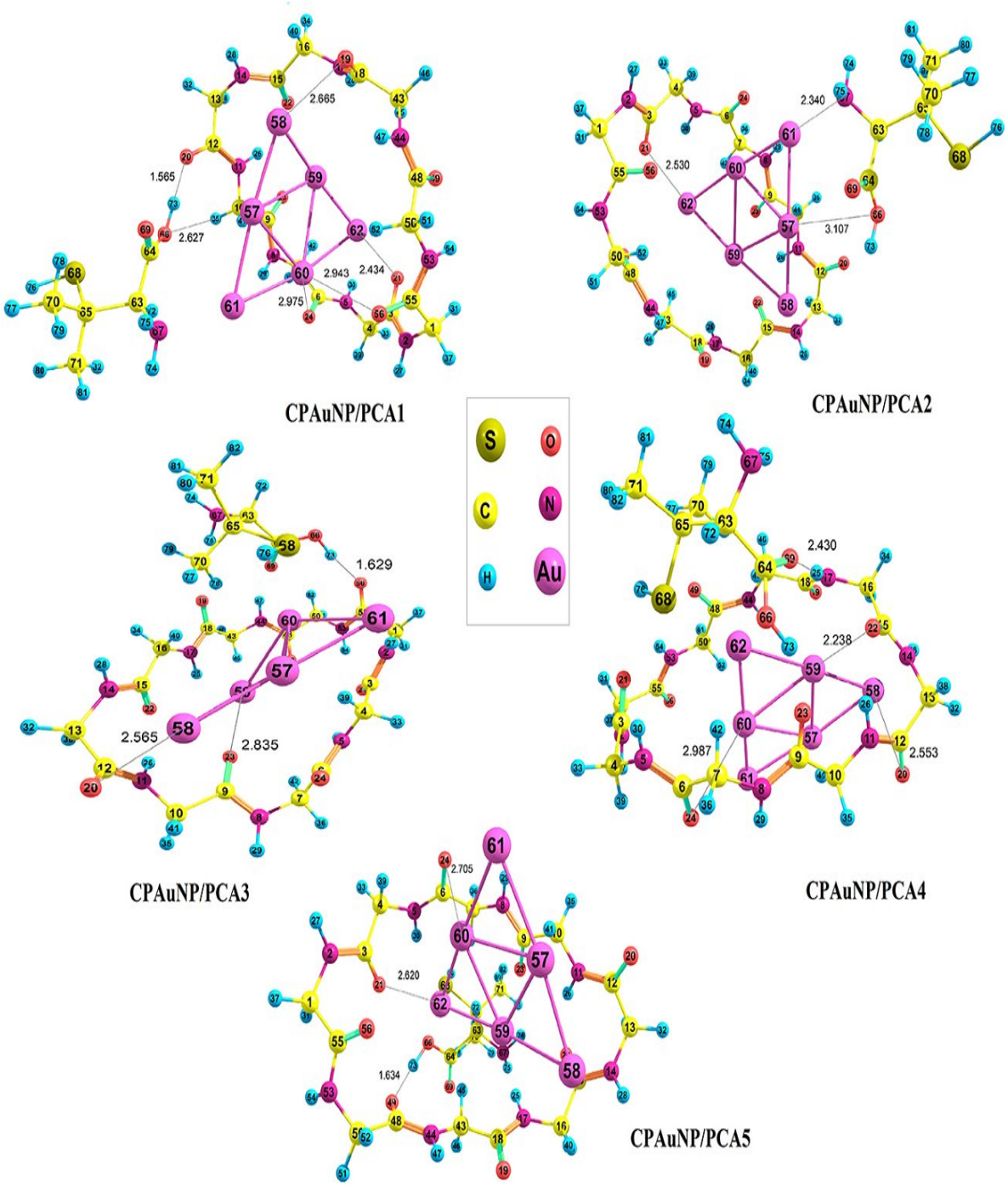

Figure 2. Optimized structures of CPAuNP/PCA1-5 in aqueous solution at M062X/6-31G.

The binding energy magnitude reveals that the structures have stability in that the interactions of PCA with CP and AuNP creates intermolecular hydrogen bonds along with more and stronger interactions in Au-L (L=H, O, S, C, N), thus making CPAuNP/PCA1, 4, and 9 more stable in water in water. Regarding the most stable configuration of CPAuNP/PCA1, the PCA drug structure is separately optimized adjacent to CP and AuNP. CP/PCA and AuNP/PCA structures are shown in Table 1 and Fig. 1.

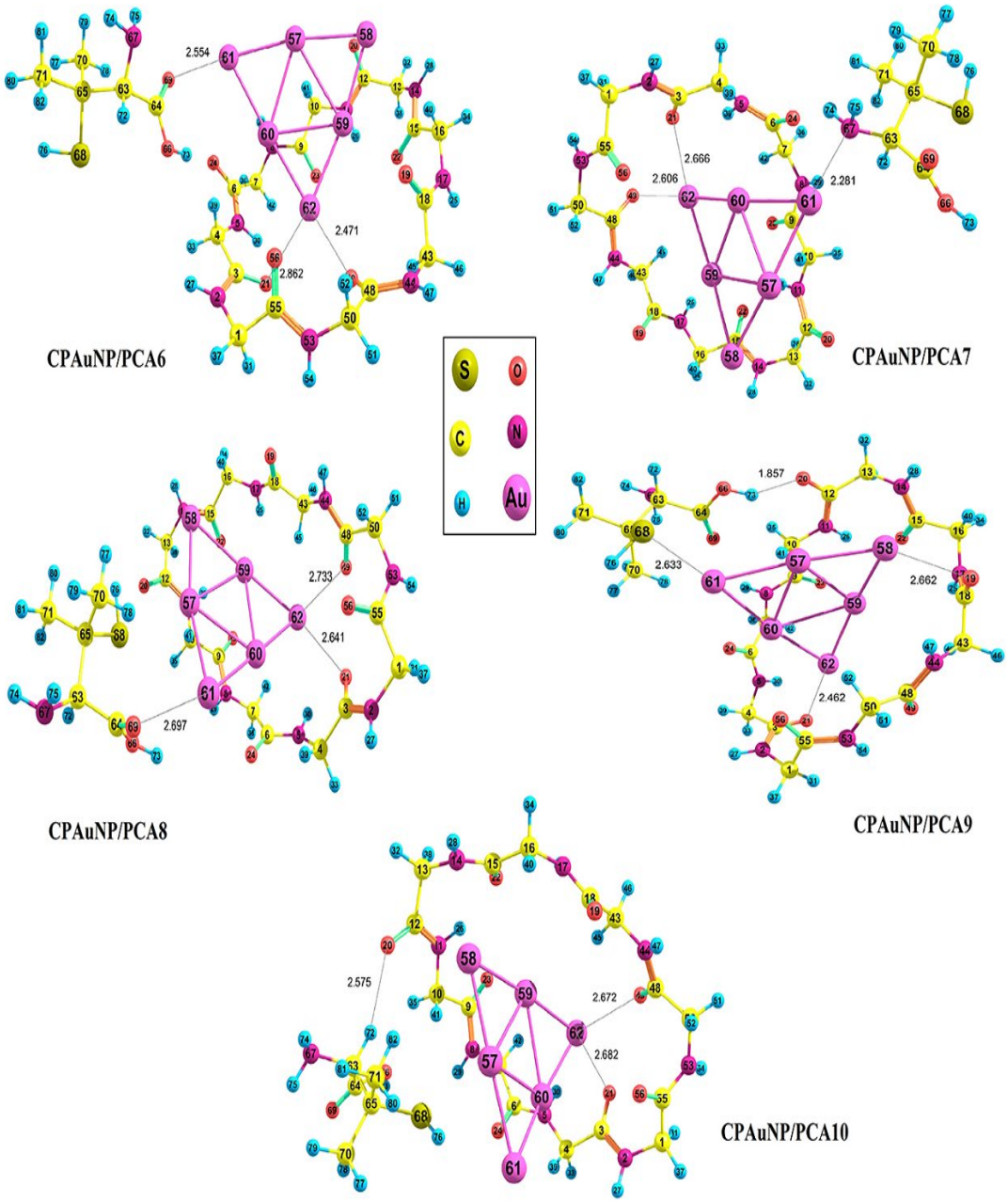

Figure 3. Optimized structures of CPAuNP/PCA6-10 in aqueous solution at M062X/6-31G**.

In this study, the solvation energies (ΔE_{solv}) were evaluated for all configurations (Table 1). The obtained values are negative, indicating that the solvation process is favourable. Increasing the solubility of the drug next to the carrier is one of the most important factors in choosing the appropriate carrier. In our studied drug delivery system, the solubility of the PCA drug is increased from -31.35 kJ mol^{-1} to -138.51 kJ mol^{-1} (on average for CPAuNP/PCA1-10). Therefore, CPAuNP can be an effective carrier for PCA drug. The important characteristic of CP is possessing NH and CO functional groups, creating hydrogen bond between PCA drug, CPAuNP carrier and solvent molecules. The presence of AuNP increases the binding energy, while cyclic peptide increases solubility. Therefore, CP and AuNP complement each other, creating a better carrier enjoying better features.

The chemical reactivity and stability were studied by E_g (the energy gap between LUMO and HOMO) and quantum molecular descriptors such as electrophilicity index (ω) and global hardness (η). The higher the amount of ω, the lower the amount of η, which is defined as the

resistance of a chemical specie against a change in its electron structure. Therefore, the stability reduces while the reactivity increases (Table 2). PCA and CP in the aqueous solution enjoy high η values of 4.68 *eV* and 4.95 *eV*, with a relatively high stability index. However, compared to PCA and CP, AuNP enjoys a higher index of reactivity mainly due to its hardness value of 2.69 *eV* and its gap energy of 5.38 *eV*. For CPAuNP/PCA1-10 configurations, the E_g and η values obtained are lower than those for CP and PCA drug, that showing the increase of the reactivity of CP and penicillamine drug for all configurations in both phases. As shown in Table 2, ω values in AuNP is higher than those in PCA drug and CPAuNP/PCA1-10 in both aqueous solution and gas phase indicating that AuNP plays as an electron receptor.

Table 2. Quantum molecular descriptors (*eV*) for all structures.

Species	E_{LUMO}	E_{HOMO}	E_g	η	ω
		H_2O			
PCA	1.21	-8.16	9.37	4.68	1.28
CP	1.40	-8.50	9.89	4.95	1.28
AuNP	-1.56	-6.93	5.38	2.69	3.35
CP/ PCA	0.92	-8.02	8.94	4.47	1.41
AuNP/ PCA	-1.54	-6.61	5.07	2.53	3.28
CPAuNP/ PCA1	-1.11	-6.39	5.28	2.64	2.66
CPAuNP/ PCA2	-1.42	-6.53	5.10	2.55	3.10
CPAuNP/ PCA3	-1.30	-6.35	5.04	2.52	2.91
CPAuNP/ PCA4	-1.40	-6.53	5.13	2.56	3.07
CPAuNP/ PCA5	-1.48	-6.64	5.15	2.57	3.20
CPAuNP/ PCA6	-1.32	-6.57	5.24	2.62	2.97
CPAuNP/ PCA7	-1.40	-6.43	5.03	2.51	3.05
CPAuNP/ PCA8	-1.42	-6.39	4.96	2.48	3.07
CPAuNP/ PCA9	-1.20	-6.38	5.18	2.59	2.77
CPAuNP/ PCA10	-1.41	-6.57	5.16	2.58	3.09
		gas			
PCA	1.34	-8.02	9.36	4.68	1.18
CP	1.34	-8.58	9.92	4.96	1.32
AuNP	-2.32	-7.56	5.24	2.62	4.65
CP/ PCA	0.80	-8.14	8.94	4.47	1.50
AuNP/ PCA	-1.82	-6.78	4.95	2.47	3.74
CPAuNP/ PCA1	-1.19	-6.20	5.01	2.50	2.73
CPAuNP/ PCA2	-1.30	-6.13	4.84	2.42	2.84
CPAuNP/ PCA3	-1.23	-6.23	4.99	2.50	2.80
CPAuNP/ PCA4	-1.23	-6.38	5.14	2.57	2.82
CPAuNP/ PCA5	-1.38	-6.42	5.04	2.52	3.03
CPAuNP/ PCA6	-1.56	-6.58	5.01	2.50	3.31
CPAuNP/ PCA7	-1.45	-6.39	4.93	2.46	3.12
CPAuNP/ PCA8	-1.51	-6.28	4.76	2.38	3.19
CPAuNP/ PCA9	-1.30	-6.19	4.89	2.44	2.87
CPAuNP/ PCA10	-1.71	-6.54	4.83	2.41	3.53

In this section, QTAIM analysis is used to run a comprehensive study on the inter-molecular interactions. The molecular electronic charge density $\rho(r)$ and its Laplacian $\nabla^2\rho(r)$ correspond to the strength and characteristic of a bond, respectively. The higher the value of $\rho(r)$ the stronger the bond. Moreover, $\nabla^2\rho$ and H_b provide more information concerning the nature of the interactions. When ($\nabla^2\rho < 0$, $H_b < 0$), ($\nabla^2\rho > 0$, $H_b < 0$) and ($\nabla^2\rho > 0$, $H_b > 0$), the interactions are strong, moderate and weak, respectively [34]. The parameter $-G_b/V_b$ if $-G_b/V_b > 1$, $0.5 < -G_b/V_b < 1$ and $-G_b/V_b < 0.5$ would be noncovalent, partially covalent and covalent bonds, respectively.

As the results of the DFT calculations revealed, from among the various configurations,

the CPAuNP/PCA1 structure was found to be the most stable while CPAuNP/PCA10 is the most unstable. The values of $\nabla^2\rho$ are positive, so the Au-Au interactions have the electrostatic nature. Even for the closed shell interactions, negative H_b values indicate a covalent bond [35]. As shown in Table 3, the Au-Au interactions in AuNP, with values of $\nabla^2\rho > 0$, $H_b < 0$ and $0.5 < -G_b/V_b < 1$ show partially covalent bonds. In addition, for other CPAuNP/PCA2-10 structures, the Au-Au interactions are found to be the same. The values obtained from H_b, $-G_b/V_b$, V_b, G_b, $\nabla^2\rho(r)$ and $\rho(r)$ for CPAuNP/PCA1 are shown in Table 3. The molecular graph for the most stable state in the aqueous solution is also presented in Fig. 4. $E_{HB} = 1/2\, V_b$ can be employed to calculate Hydrogen bonding energy [36].

Table 3. Topological parameters in *a.u.* for CPAuNP/PCA1.

Atoms	$\rho(r)$	$\nabla^2\rho(r)$	V_b	G_b	$-G_b/V_b$	H_b
			Au-Au interactions			
Au60 - Au62	0.0340	0.0891	-0.0351	0.0287	0.8177	-0.0064
Au58 - Au59	0.0380	0.0948	-0.0401	0.0319	0.7956	-0.0082
Au59 - Au60	0.0270	0.0779	-0.0249	0.0222	0.8912	-0.0027
Au57 - Au59	0.0294	0.0849	-0.0289	0.0251	0.8671	-0.0038
Au57 - Au58	0.0627	0.1280	-0.0742	0.0531	0.7157	-0.0211
Au57 - Au60	0.0407	0.1018	-0.0440	0.0347	0.7890	-0.0093
Au57 - Au61	0.0440	0.1020	-0.0481	0.0368	0.7653	-0.0113
Au60 - Au61	0.0649	0.1084	-0.0725	0.0498	0.6870	-0.0227
Au59 - Au62	0.0670	0.1231	-0.0776	0.0542	0.6982	-0.0234
			Au-L interactions			
C6 - Au62	0.0076	0.0259	-0.0039	0.0052	1.3375	0.0013
H41 - Au59	0.0070	0.0240	-0.0037	0.0048	1.3216	0.0012
H41 - Au57	0.0110	0.0360	-0.0068	0.0079	1.1585	0.0011
O21 - Au62	0.0406	0.1799	-0.0495	0.0473	0.9538	-0.0023
N11 - Au59	0.0080	0.0235	-0.0048	0.0054	1.1075	0.0005
N8 - Au60	0.0077	0.0246	-0.0042	0.0052	1.2297	0.0010
N17 - Au59	0.0071	0.0192	-0.0037	0.0043	1.1405	0.0005
N14 - Au58	0.0084	0.0227	-0.0046	0.0051	1.1145	0.0005
N44 - Au59	0.0097	0.0266	-0.0058	0.0062	1.0728	0.0004
N53 - Au62	0.0080	0.0237	-0.0048	0.0053	1.1209	0.0006
O20 - Au57	0.0048	0.0142	-0.0024	0.0030	1.2564	0.0006
O19 - Au58	0.0272	0.1031	-0.0284	0.0271	0.9532	-0.0013
C9 - Au59	0.0058	0.0176	-0.0026	0.0035	1.3347	0.0009
O22 - Au59	0.0076	0.0242	-0.0047	0.0054	1.1379	0.0007
O24 - Au60	0.0153	0.0538	-0.0131	0.0133	1.0128	0.0002
O56 - Au60	0.0160	0.0572	-0.0139	0.0141	1.0135	0.0002
O49 - Au62	0.0075	0.0235	-0.0041	0.0050	1.2097	0.0009
H52 - Au62	0.0071	0.0202	-0.0033	0.0042	1.2771	0.0009
Au57 - O69	0.0090	0.0299	-0.0062	0.0069	1.1012	0.0006
Au61 - N67	0.0611	0.2368	-0.0765	0.0678	0.8869	-0.0087
			Intermolecular hydrogen bonds			
H35 - O66	0.0079	0.0316	-0.0052	0.0065	1.2652	0.0014
O20 - H73	0.0603	0.1581	-0.0537	0.0466	0.8679	-0.0071

In the CPAuNP/PCA1-10 configurations, two important categories of interactions were observed: The first category includes interactions between AuNP and CP, or AuNP, and the PCA drug. These interactions are of Au-L type, where L contains (L = H, O, S, C, N). However, when there are more Au-L interactions with higher $\rho(r)$ and $\nabla^2\rho(r)$ values, the configuration enjoys more stability. The CPAuNP/PCA1 structure shows 20 Au-L interactions with $\rho_{av} = 0.0138$ and $\nabla^2\rho_{av} = 0.0493$ (on average). As

shown in Table 3, for CPAuNP/PCA1, 17 Au-L interactions are considered weak interactions with $H_b > 0$, $\nabla^2\rho > 0$ and $-G_b/V_b > 1$ while the remaining 3 Au-L interactions are partially covalent interactions with $0.5 < -G_b/V_b < 1$, $H_b < 0$ and $\nabla^2\rho > 0$. The second category of interactions includes those between PCA drug and CP via the hydrogen bond. The bond H73...O20 with E_{HB} = -79.49 kJ mol^{-1} and $0.5 < -G_b/V_b < 1$, $H_b < 0$ and $\nabla^2\rho > 0$ is considered as the medium hydrogen bond, while H35...O66 is another hydrogen bond with $H_b > 0$, $\nabla^2\rho > 0$ and $-G_b/V_b > 1$ considered as the weak hydrogen bond.

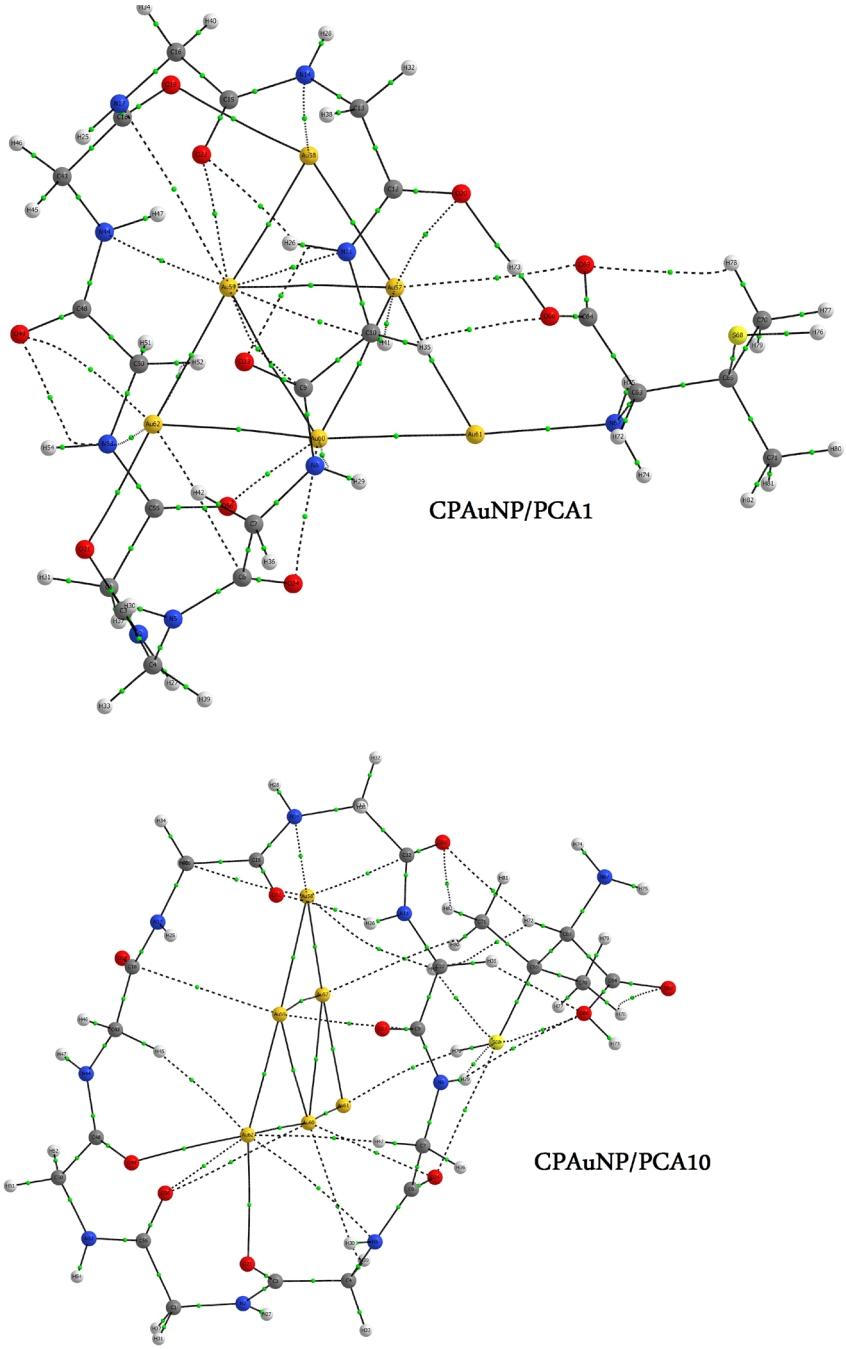

Figure 4. Molecular graphs of CPAuNP/PCA1 and CPAuNP/PCA10 in aqueous solution at M062X/6-31G**. Small green spheres and lines related to the bond critical points (BCP) and the bond paths, respectively.

Table 4. Topological parameters in *a.u.* for CPAuNP/PCA10

Atoms	ρ(r)	$\nabla^2\rho$(r)	V_b	G_b	-G_b/V_b	H_b
			Au-Au interactions			
Au60 - Au62	0.0515	0.1100	-0.0579	0.0427	0.7374	-0.0152
Au58 - Au59	0.0446	0.1051	-0.0494	0.0378	0.7658	-0.0116
Au59 - Au62	0.0585	0.1123	-0.0659	0.0470	0.7129	-0.0189
Au57 - Au59	0.0271	0.0779	-0.0249	0.0222	0.8908	-0.0027
Au57 - Au58	0.0594	0.1246	-0.0697	0.0504	0.7234	-0.0193
Au59 - Au60	0.0376	0.0983	-0.0400	0.0323	0.8076	-0.0077
Au57 - Au60	0.0337	0.0946	-0.0355	0.0296	0.8326	-0.0060
Au57 - Au61	0.0504	0.1113	-0.0570	0.0424	0.7443	-0.0146
Au60 - Au61	0.0509	0.1142	-0.0582	0.0434	0.7453	-0.0148
			Au-L interactions			
O23 - Au59	0.0077	0.0274	-0.0041	0.0055	1.3349	0.0014
C12 - Au58	0.0101	0.0380	-0.0063	0.0079	1.2525	0.0016
N5 - Au62	0.0087	0.0241	-0.0050	0.0055	1.0984	0.0005
N14 - Au58	0.0189	0.0582	-0.0155	0.0150	0.9700	-0.0005
O24 - Au60	0.0143	0.0492	-0.0116	0.0120	1.0298	0.0003
O19 - Au59	0.0076	0.0271	-0.0041	0.0054	1.3278	0.0013
O21 - Au62	0.0257	0.0975	-0.0268	0.0256	0.9548	-0.0012
O56 - Au62	0.0107	0.0355	-0.0077	0.0083	1.0780	0.0006
H40 - Au58	0.0070	0.0232	-0.0034	0.0046	1.3514	0.0012
H41 - Au58	0.0055	0.0152	-0.0024	0.0031	1.2905	0.0007
H45 - Au62	0.0085	0.0289	-0.0046	0.0059	1.2861	0.0013
H39 - Au60	0.0063	0.0215	-0.0032	0.0043	1.3509	0.0011
O56 - Au60	0.0085	0.0275	-0.0055	0.0062	1.1202	0.0007
H42 - Au62	0.0065	0.0194	-0.0029	0.0039	1.3481	0.0010
O49 - Au62	0.0270	0.1016	-0.0280	0.0267	0.9537	-0.0013
Au61 - H76	0.0095	0.0259	-0.0046	0.0055	1.2005	0.0009
Au57 - H80	0.0064	0.0206	-0.0030	0.0041	1.3550	0.0011
			Intermolecular hydrogen bonds			
H35 - O66	0.0107	0.0367	-0.0078	0.0085	1.0894	0.0007
O20 - H72	0.0083	0.0266	-0.0054	0.0060	1.1135	0.0006
H29 - O66	0.0045	0.0203	-0.0030	0.0040	1.3458	0.0010
O20 - H82	0.0040	0.0154	-0.0022	0.0030	1.3849	0.0008

The structure of CPAuNP/PCA10 is found to be the most unstable configuration. Fig. 4 and Table 4 show the molecular graph and the values of V_b, G_b, H_b, $\nabla^2\rho(r)$, ρ(r) and $-G_b/V_b$ in solution phase of this configuration. The interactions of Au-L with $0.5 < -G_b/V_b < 1$, $H_b < 0$ and $\nabla^2\rho > 0$ such as CPAuNP/PCA1 are partially covalent interactions. CPAuNP/PCA10 shows 3 Au-L interactions with moderate effect, along with 14 weak interactions. This structure has 3 Au-L interactions fewer than the most stable configuration, i.e., CPAuNP/PCA1. CPAuNP/PCA10 structure shows 17 Au-L interactions with $\rho_{av} = 0.0111$ and $\nabla^2\rho_{av} = 0.0376$ (on average). Moreover, there are 4 hydrogen bonds in this structure, namely, H35...O66, H72...O20, H29...O66 and H82...O20 which show weak interactions. The values of V_b, G_b, H_b, $\nabla^2\rho(r)$, ρ(r) and $-G_b/V_b$ along with medium hydrogen bonds or Au-L were studied in the other structures. The results obtained are presented in Table 5.

In the CPAuNP/PCA2 structure, the PCA drug has interaction just with AuNp, indicating that there is no hydrogen bond between CP and PCA. CPAuNP/PCA2 is an unstable structure in which the PCA is perpendicular to CPAuNP, with the drug approaching AuNP from the NH_2 and OH groups side. This structure has 2 medium Au-L interactions, and 17 weak interactions with $\rho_{av} = 0.0121$ and $\nabla^2\rho_{av} = 0.0424$. CPAuNP/PCA4 is the second stable configuration, containing 20 weak Au-L interactions and 1 intermediate interaction

with $\rho_{av} = 0.0111$ and $\nabla^2\rho_{av} = 0.0343$, along with 5 weak hydrogen bonds. Although the number of hydrogen bonds in CPAuNP/PCA1 is lower than those in CPAuNP/PCA4, it enjoys a comparatively higher stability compared to CPAuNP/PCA4 in that it has more and stronger Au-L interactions.

Table 5. Topological parameters (medium interactions) in *a.u.* for CPAuNP/PCA2-9.

Atoms	ρ(r)	$\nabla^2\rho$(r)	V_b	G_b	$-G_b/V_b$	H_b
			CPAuNP/PCA1			
O21 - Au62	0.0406	0.1799	-0.0495	0.0473	0.9538	-0.0023
O19 - Au58	0.0272	0.1031	-0.0284	0.0271	0.9532	-0.0013
Au61 - N67	0.0611	0.2368	-0.0765	0.0678	0.8869	-0.0087
O20 - H73	0.0603	0.1581	-0.0537	0.0466	0.8679	-0.0071
			CPAuNP/PCA2			
O21 - Au62	0.0338	0.1394	-0.0388	0.0368	0.9498	-0.0019
Au61 - N67	0.0625	0.2447	-0.0790	0.0701	0.8870	-0.0089
			CPAuNP/ PCA3			
O23 - Au59	0.0195	0.0717	-0.0182	0.0181	0.9924	-0.0001
O20 - Au58	0.0325	0.1285	-0.0363	0.0342	0.9420	-0.0021
O49 - Au62	0.0371	0.1519	-0.0434	0.0407	0.9373	-0.0027
Au60 - S68	0.0614	0.1543	-0.0681	0.0533	0.7832	-0.0148
			CPAuNP/ PCA4			
Au62 - S68	0.0529	0.1395	-0.0577	0.0463	0.8022	-0.0114
			CPAuNP/ PCA5			
O21 - Au62	0.0291	0.1121	-0.0314	0.0297	0.9460	-0.0017
Au62 - O66	0.0297	0.1137	-0.0327	0.0305	0.9353	-0.0021
H25 - N67	0.0243	0.0581	-0.0167	0.0156	0.9357	-0.0011
O49 - H73	0.0487	0.1550	-0.0406	0.0397	0.9768	-0.0009
			CPAuNP/ PCA6			
O21 - Au62	0.0186	0.0659	-0.0172	0.0169	0.9783	-0.0004
O49 - Au62	0.0378	0.1633	-0.0450	0.0429	0.9534	-0.0021
O56 - Au62	0.0179	0.0638	-0.0161	0.0160	0.9970	-0.0004
Au61 - O69	0.0324	0.1322	-0.0366	0.0348	0.9511	-0.0018
O24 - H73	0.0629	0.1598	-0.0574	0.0486	0.8481	-0.0087
			CPAuNP/ PCA7			
O49 - Au62	0.0301	0.1167	-0.0327	0.0310	0.9457	-0.0018
O21 - Au62	0.0265	0.1012	-0.0278	0.0265	0.9554	-0.0012
Au61 - N67	0.0705	0.2823	-0.0928	0.0817	0.8803	-0.0111
			CPAuNP/ PCA8			
O21 - Au62	0.0276	0.1067	-0.0295	0.0281	0.9516	-0.0014
O49 - Au62	0.0240	0.0891	-0.0240	0.0232	0.9633	-0.0009
Au57 - S68	0.0250	0.0724	-0.0210	0.0195	0.9316	-0.0014
Au61 - O69	0.0256	0.0963	-0.0264	0.0253	0.9557	-0.0012
			CPAuNP/ PCA9			
O19 - Au58	0.0272	0.1038	-0.0286	0.0273	0.9531	-0.0010
O21 - Au62	0.0389	0.1665	-0.0465	0.0441	0.9477	-0.0020
Au61 - S68	0.0529	0.1403	-0.0578	0.0465	0.8034	-0.0110
			CPAuNP/ PCA10			
N14 - Au58	0.0189	0.0582	-0.0155	0.0150	0.9700	-0.0005
O21 - Au62	0.0257	0.0975	-0.0268	0.0256	0.9548	-0.0012
O49 - Au62	0.0270	0.1016	-0.0280	0.0267	0.9537	-0.0013

A similar argument can be made for CPAuNP/PCA9, which is the third stable configuration. This structure has 3 intermediate interactions and 17 weak Au-L interactions with $\rho_{av} = 0.0132$ and $\nabla^2\rho_{av} = 0.0429$, along with 3 weak hydrogen bonds. Compared to

CPAuNP/PCA1, this configuration has weaker inter-molecular interactions (Table 5). The order of stability of other configurations is as follows: CPAuNP/PCA3 (has 4 Au-L medium interactions and 12 weak interactions with $\rho_{av}=0.0151$ and $\nabla^2\rho_{av}=0.0487$ and 5 weak hydrogen bonds) > CPAuNP/PCA7 (has 3 Au-L medium interactions and 13 weak interactions with $\rho_{av}=0.0143$ and $\nabla^2\rho_{av}=0.0512$ and 2 weak hydrogen bonds) > CPAuNP/PCA5 (has 2 medium interactions of Au-L and 15 weak interactions, with the values of $\rho_{av}=0.0111$ and $\nabla^2\rho_{av}=0.0375$, in this structure existes 2 medium hydrogen bonds and 6 weak hydrogen bonds) > CPAuNP/PCA6 (has 4 Au-L medium interactions and 11 weak interactions with $\rho_{av}=0.0134$ and $\nabla^2\rho_{av}=0.0482$, and 1 medium hydrogen bond and 1 weak one) > CPAuNP/PCA8 (has 4 Au-L medium interactions and 17 weak ones with $\rho_{av}=0.0112$ and $\nabla^2\rho_{av}=0.0379$, and 1 weak hydrogen bond).

3. Material and Methods

In the present study, all the analysis and calculations were performed at the M06-2X density functional level of theory by GAUSSIAN 09 software [37, 38]. The structure of penicillamine (PCA) drug, cyclic peptide (CP), gold nanoparticles (AuNP) and ten configurations of CPAuNP/PCA1-10 was optimized using the basis set 6-31G(d,p). Moreover, the LANL2DZ basis set was used for the gold [39]. The polarized continuum model (PCM) was employed to examine the solvent effects (water) [40, 41]. Solvation energy was calculated using the following equation:

$$\Delta E_{solv}=E_{sol}-E_{gas} \quad (2)$$

Where E_{sol} and E_{gas} stand for the energy of structures in solution and gas phases, respectively. Electronic energies (local minimum on the potential energy surface) were used to calculate the binding and solvation energies.

Quantum molecular descriptors, such as global hardness and electrophilicity index, can be used to describe the chemical reaction and the stability constant. Global hardness (η), which refers to the resistance a molecule shows against a change in its electronic structure, can be calculated through the following formula:

$$\eta=(I-A)/2 \quad (3)$$

In which $I=-E_{HOMO}$ and $A=-E_{LUMO}$ are the ionization energy and the electron affinity of a molecule, respectively [42,43]. The energy difference between LUMO (lowest unoccupied molecular orbital) and HOMO (highest occupied molecular orbital), the highest molecular energy, is shown as E_g, which is an index of system stability and reduced reactivity. Electrophilicity index (ω) is determined using the following equation by Parr [44].

$$\omega=(I+A)^2/8\eta \quad (4)$$

In the quantum theory of atoms in molecules (QTAIMs), Bond Critical Points (BCP) can be used as a basis to describe the nature and power of bonding interactions. The AIMAll software was employed to perform all AIM calculations [45, 46]. The QTAIMs calculations create a link between the basic concepts of chemistry and those of quantum mechanics through the analysis of electron density topology [47]. The magnitude of various electron density, presented as $\rho(r)$, including potential energy density (V_b), the kinetic energy density (G_b), the total energy density (H_b) and the Laplacian of the electron density $(\nabla^2\rho)$ in bond critical points were examined and used as a basis to make comparisons between the nature of the bonds in different structures.

4. Conclusions

In this study, 10 gold nanoparticle-cyclic peptide configurations with anticancer penicillamine PCA drug were examined in aqueous solution and gas phase at M06-2X level. The observed binding energy values is indicative of the fact that CPAuNP showed an appropriate function when used with PCA drug in (CPAuNP/PCA1-10), with the simultaneous interaction of the drug with CP and AuNP resulting in higher stability. The results of the analysis of the solvent energies show that the solubility of PCA and AuNP increases in the presence of CP.

Moreover, the PCA drug has generally high indexes of Global hardness (η) and energy gap (E_g), however, when it is in the presence of AuNP and CP, these rates show a decrease, which is indicative of the reactivity of PCA with CPAuNP. According to the AIM studies, the PCA drug can interact with CPAuNP as Au-L (L = N, O, S, C, H) and hydrogen bond. Most of the Au-L interactions are weak. The AIM results showed that, in the most stable configuration of CPAuNP/PCA1, there are more and stronger Au-L interactions, and powerful hydrogen bonds.

Acknowledgments

We thank the Research Center for Animal Development Applied Biology for allocation of computer time.

References and Notes

[1] Zhuang, C.; Guan, X.; Ma, H.; Cong, H.; Zhang, W.; Miao, Z. *Eur. J. Med. Chem.* **2019,** *163*, 883. [Crossref]

[2] Hossen, S.; Hossain, M. K.; Basher, M.; Mia, M.; Rahman, M.; Uddin, M. J. *J. Adv. Res.* **2019,** *15*, 1. [Crossref]

[3] Guo, S.; Wang, E. *Nano Today*. **2011**, 6, 240. [Crossref]

[4] Lohse, S. E.; Murphy C. J. *J. Am. Chem. Soc*. **2012**, *134*, 15607. [Crossref]

[5] Khanyile, N.; Krause R.; Vilakazi, S.; Torto, N. *S. Afr. J. Chem*. **2019**, *72*, 207. [Crossref]

[6] Parboosing, R.; Govender, T.; Maguire G. E.; Kruger HG. *S. Afr. J. Chem*. **2018**, *71*, 1. [Crossref]

[7] Lal, S.; Clare, S. E.; Halas, N. J. *Acc. Chem. Res*. **2008**, *41*, 1842. [Crossref]

[8] Boisselier, E.; Astruc, D. *Chem. Soc. Rev*. **2009**, *38*, 1759. [Crossref]

[9] Nasrolahi Shirazi, A.; Mandal, D.; Tiwari, R. K.; Guo, L.; Lu, W.; Parang, K. *Mol. Pharmaceut*. **2013**, *10*, 500. [Crossref]

[10] Joo, S. H. *Biomol. Ther*. **2012**, *20*, 19. [Crossref]

[11] Rezai, T.; Yu, B.; Millhauser, G. L.; Jacobson, M. P.; Lokey, R. S. *J. Am. Chem. Soc*. **2006**, *128*, 2510. [Crossref]

[12] Brea, R. J.; Reiriz, C.; Granja, J. R. *Chem. Soc. Rev*. **2010**, *39*, 1448. [Crossref]

[13] Tambunan, U. S. F.; Alkaff A. H.; Nasution M. A. F.; Parikesit A. A.; Kerami D. *J. Mol. Graph. Model*. **2017**, *74*, 366. [Crossref]

[14] García-Gallego, S.; Franci, G.; Falanga, A.; Gómez, R.; Folliero, V.; Galdiero, S. *Molecules* **2017**, *22*, 1581. [Crossref]

[15] Larnaudie, S. C.; Brendel, J. C.; Romero-Canelón, I.; Sanchez-Cano, C.; Catrouillet, S.; Sanchis, J. *Biomacromolecules* **2018**, *19*, 239. [Crossref]

[16] Dartois, V.; Sanchez-Quesada, J.; Cabezas E.; Chi, E.; Dubbelde, C.; Dunn, C. *Antimicrob. Agents Chemother*. **2005**, *49*, 3302. [Crossref]

[17] Khalfa, A.; Tarek, M. *J. Phys. Chem*. **2010**, *114*, 2676. [Crossref]

[18] Lebogang, L.; Hedström, M.; Mattiasson, B. *Anal. Chim. acta*. **2014**, *826*, 69. [Crossref]

[19] Guida, F.; Battisti, A.; Gladich, I.; Buzzo, M.; Marangon, E.; Giodini, L. *Biosens. Bioelectron*. **2018**, *100*, 298. [Crossref]

[20] Hruby, V. J. *Pept. Sci*. **2016**, *106*, 884. [Crossref]

[21] Khavani. M.; Izadyar. M.; Housaindokht M. R. *J. Mol. Graph. Model*. **2017**, *71*, 28. [Crossref]

[22] Kamel, M.; Raissi, H.; Morsali, A.; Shahabi, M. *Appl. Surf. Sci*. **2018**, *434*, 492. [Crossref]

[23] Teymoori, M.; Morsali, A.; Bozorgmehr, M. R.; Beyramabadi, S. A. *Bull. Korean. Chem. Soc*. **2017**, *38*, 869. [Crossref]

[24] Ghaleb, A.; Aouidate, A.; Sbai, A.; Lakhlifi, T.; Maghat, H.; Bouachrine, M. *Orbital: Electron. J. Chem.* **2017**, *9*, 337. [Crossref]

[25] Avarand, S.; Morsali, A.; Heravi, M. M.; Beyramabadi S. A. *Orbital: Electron. J. Chem.* **2019**, *11*, 161. [Crossref]

[26] Nasrabadi, M.; Beyramabadi, S. A.; Morsali, A. *Int. J. Biol. Macromol.* **2020,** *147*, 534. [Crossref]

[27] Rahbar, M.; Morsali, A.; Bozorgmehr, M. R.; Beyrmabadi, S. A. *J. Mol. Liq.* **2020,** *302*, 112495. [Crossref]

[28] Naghavi, F.; Morsali, A.; Bozorgmehr, M. R.; Beyramabadi, S. A. *J. Mol. Liq.* **2020**, 719, 12. [Crossref]

[29] Shabani, Z.; Morsali, A.; Bozorgmehr, M. R.; Beyramabadi, S. A. *Chem. Phys. Lett.* **2019,** *719*, 12. [Crossref]

[30] El Alamy, A.; Amine, A.; Bouachrine, M. *Orbital: Electron. J. Chem.* **2017,** *9*, 188. [Crossref]

[31] Shaki, H.; Morsali, A.; Raissi, H.; Hakimi, M.; Beyramabadi, S. A. *J. Serb. Chem. Soc.* **2018**, *83*, 167. [Crossref]

[32] Naghavi, F.; Morsali, A.; Bozorgmehr, M. R. *J. Mol. Liq*. **2019,** *282*, 392. [Crossref]

[33] Khorrampour, R.; Raissi, H.; Shaki, H.; Morsali, A.; Hashemzadeh, H. *Mol. Simulat.* **2020,** *46*, 408. [Crossref]

[34] Rozas, I.; Alkorta, I.; Elguero, J. *J. Am. Chem. Soc*. **2000**, *122*, 11154. [Crossref]

[35] Espinosa, E.; Alkorta, I.; Elguero, J.; Molins, E. *J. Chem. Phys*. **2002**, *117*, 5529. [Crossref]

[36] Espinosa, E.; Souhassou, M.; Lachekar, H.; Lecomte, C. *Acta Crystallogr B*. **1999**, *55*, 563. [Crossref]

[37] Zhao, Y.; Truhlar, D. G. *J. Chem. Phys*. **2006**, *125*, 194101. [Crossref]

[38] Frisch, M.; Trucks, G.; Schlegel, H.; Scuseria, G.; Robb, M.; Cheeseman, J.; Scalmani, G.; Barone, V.; Mennucci, B.; Petersson, G. Gaussian 09, revision B.01. Gaussian, Inc., Wallingford, CT 2009. [Link]

[39] Hay, P. J.; Wadt, W. R. *J. Chem. Phys*. **1985**, *82*, 270. [Crossref]

[40] Tomasi, J.; Persico, M. *Chem. Rev*. **1994**, *94*, 2027. [Crossref]

[41] Cammi, R.; Tomasi, J. *J. Comput. Chem*. **1995**, *16*, 1449. [Crossref]

[42] Srivastava, A.; Mishra, R.; Joshi, B.; Gupta, V.; Tandon, P. *Mol. Simulat*. **2014**, *40*, 1099. [Crossref]

[43] Domingo, L. R.; Aurell, M. J.; Pérez, P.; Contreras, R. *J. Phys. Chem*. **2002**, *106*, 6871. [Crossref]

[44] Parr, R. G.; Szentpaly, Lv.; Liu, S. *J. Am. Chem. Soc*. **1999**, *121*, 1922. [Crossref]

[45] Keith, T. A. AIMAII (Version 13.05. 06).; TK Gristmill Software, Overland Park.; KS.; USA.; 2013. [Link]

[46] do Rego, D. G.; de Oliveira, B. G. *Orbital: Electron. J. Chem.* **2016**, *1*, 1. [Crossref]

[47] Bader, R. F. *Chem. Rev*. **1991**, *91*, 893. [Crossref]